Condensation Heat Transfer and Pressure Drop of R-134a in the Oblong Shell and Plate Heat Exchanger

Jae-Hong Park†, Young-Soo Kim*

Department of Refrigeration and Air-Conditioning Engineering, Pukyong University, Busan 608-739, Korea

**College of Engineering, School of Mechanical Engineering, Pukyong University, Busan 608-739, Korea*

Key words: Oblong shell and plate heat exchanger, Condensation, R-134a, Heat transfer, Pressure drop

ABSTRACT: Condensation heat transfer experiments were conducted with a oblong shell and plate heat exchanger without oil in a refrigerant loop using R-134a. An experimental refrigerant loop has been developed to measure the condensation heat transfer coefficient h_r and frictional pressure drop Δp_f of R-134a in a vertical oblong shell and plate heat exchanger. Four vertical counter flow channels were formed in the oblong shell and plate heat exchanger by four plates having a corrugated sinusoid shape of a 45° chevron angle. The effects of the refrigerant mass flux, average heat flux, refrigerant saturation temperature and vapor quality were explored in detail. Similar to the case of a plate heat exchanger, even at a very low Reynolds number, the flow in the oblong shell and plate heat exchanger remains turbulent. The results indicate that the condensation heat transfer coefficients and pressure drops increase with the vapor quality. A rise in the refrigerant mass flux causes an increase in the h_r and Δp_f. Also, a rise in the average heat flux causes an increase in the h_r. But the effect of the average heat flux does not show significant effect on the Δp_f. On the other hand, at a higher saturation temperature, both the h_r and Δp_f found to be lower. Based on the present data, the empirical correlations are provided in terms of the Nusselt number and friction factor.

Nomenclature

A : heat transfer area of the plate [m^2]
b : channel spacing [m]
c_p : specific heat [J/kgK]
D_h : hydraulic diameter [m]
f : friction factor
i_{fg} : enthalpy of vaporization [J/kg]
L : length from center of inlet port to center of exit port [m]
$\dot{m}$: mass flow rate [kg/s]
Nu : Nusselt number
Pr : Prandtl number
Q : heat transfer rate [W]
Re : Reynolds number
T : temperature [℃]
U : overall heat transfer coefficient [W/m^2K]
u : velocity [m/s]
x : vapor quality

Greek symbols

Δp : pressure drop [Pa]

† Corresponding author
Tel.: +82-51-620-1503; fax: +82-51-623-8495
E-mail address: parksonforever@hanmail.net

ΔT : temperature difference [K]
ρ : density [kg/m^3]
μ : viscosity [Ns/m^2]
v : specific volume [m^3/kg]

Subscripts

eq : equivalent
f : liquid
g : vapor
i, o : at inlet and exit of test section
lat : latent heat
p : pre-heater
r : refrigerant
sat : saturation
sens : sensible heat
t : test section
tp : two-phase
w : water

1. Introduction

In view of space saving, the design of more compact heat exchangers is relatively important. Also, to meet the demand for saving energy and resources today, manufacturers are trying to enhance efficiency and reduce the size and weight of heat exchangers. Over the past decade, there has been tremendous advancement in the manufacturing technology of high efficiency heat exchangers. This has allowed the use of smaller and higher performance heat exchangers. Consequently, the use of smaller and high performance heat exchanger will become popular in the design of HVAC heat exchangers. Normally, these heat exchangers are used in the two-phase system for evaporation and condensation. In the design and analysis of the two-phase system with this heat exchanger, it is necessary to understand the heat transfer and frictional characteristics of the heat exchanger.

When compared with the well-established shell and tube heat exchangers, the plate heat exchanger shows a lot of advantages, such as high *NTU* values, compactness, low cost, multi duties and reduced fouling etc. Plate heat exchangers have been widely used in food processing, chemical reaction processes, and other industrial applications for many years. The advantage of using plate heat exchanger was clearly indicated in many studies.[1,2] In the last 30 years, plate heat exchangers have been introduced to the refrigeration and air conditioning systems as condensers or evaporators for their high efficiency and compactness.

The oblong shell and plate heat exchanger is different from the conventional plate heat exchanger. The plates that have an oblique pattern are ellipse in shape and stacked together in criss-cross pattern, which are enclosed in a cylindrical shell. The operating temperature up to 350℃, and the pressures up to 10 MPa can be achieved. Although oblong shell and plate heat exchanger looks different from the conventional rectangular plate heat exchanger, the underlying flow channel configuration is the same as the conventional plate heat exchanger. The oblong shell and plate heat exchanger is being introduced to refrigeration and air conditioning systems as condenser or evaporator for its high efficiency and compactness. However, there are little data available for the design of oblong shell and plate heat exchanger to be used as condenser and evaporator.

In this study, the characteristics of the condensation heat transfer and pressure drop for R-134a flowing in the oblong shell and plate heat exchanger were experimentally explored to set up data base for the design of the oblong shell and plate heat exchanger.

2. Experimental apparatus and method

The heat transfer plate and experimental system used to study the condensation of R-134a

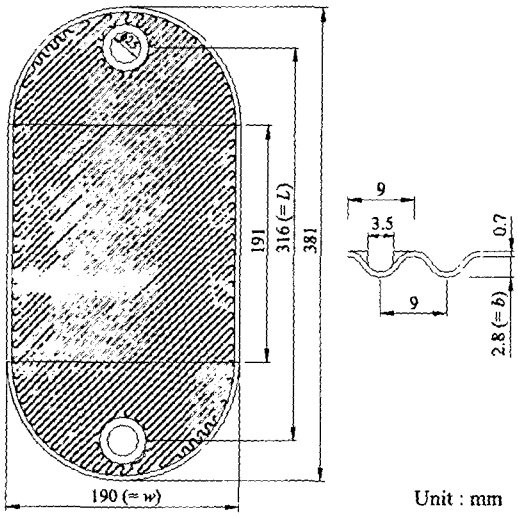

Fig. 1 Schematic diagram of heat transfer plate of oblong shell and plate heat exchanger.

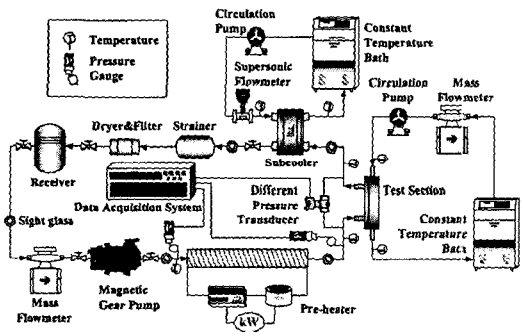

Fig. 2 Schematic diagram of two-phase flow experimental system.

are schematically shown in Figs. 1 and 2, respectively. The experimental system consisted of a test section, a refrigerant loop, a water loop and a data acquisition unit. Refrigerant R-134a is circulated in a refrigerant loop. In order to obtain different test conditions of R-134a including the vapor quality, saturation temperature (pressure) and imposed heat flux, the temperature and flow rate of the working fluid in the water loop were controlled.

2.1 Test section

The test section (oblong shell and plate heat

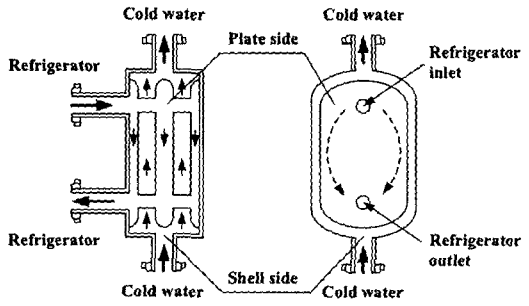

Fig. 3 Details of condensation flow direction.

exchanger) used in this study was formed by four commercialized SUS-304 plates. The plate surfaces were pressed to form grooved channels with a corrugated sinusoid shape and 45° chevron angle. The corrugated grooves on the right and left outer plates have an oblique shape but those in the middle plate have a criss-cross pattern on both sides. Due to the criss-cross pattern between two neighbor plates, the flow streams near the two plates cross each other in each channel. This cross flow creates a significant unsteady and random flow. In fact, the flow is highly turbulent even at low Reynolds number. The flow pattern of test section is schematically shown in Fig. 3.

2.2 Refrigerant loop

The refrigerant loop contains a refrigerant pump, a pre-heater, a test section, a sub-cooler, a strainer, a mass flow meter, a dryer&filter, and five sight glasses. The refrigerant pump is a magnetic pump (TUTHILL California) driven by a DC motor which is, in turn, controlled by a variable DC output motor controller. The variation of the liquid R-134a flow rate was controlled by the rotational speed of DC motor through the change of the DC current. The refrigerant flow rate was measured by a mass flow meter (Oval) installed between the pump and the receiver with an accuracy of ±0.2%.

The pre-heater is used to evaporate the refrigerant to a specified vapor quality at the test section inlet by transferring heat to R-

134a. The amount of heat transfer from the pre-heater to refrigerant is measured by a power meter (YOKOGAWA) connected to the pre-heater source. The dryer&filter intends to filter the solid particles possibly present in the loop. Meanwhile, a sub-cooler is used to condense the refrigerant vapor flowing out the test section by a cold water to avoid cavitations at the pump inlet. The pressure of the refrigerant loop can be controlled by varying the temperature and flow rate of cold water in the sub-cooler. After condensed, the sub-cooled liquid refrigerant flows back to the receiver.

2.3 Water loop for test section

The water loop in the system, which is designed for circulating cold water through the test section, has a 200 liter constant temperature water bath equipped with a 5 kW heater and an air cooled refrigerant unit of 1 RT cooling capacity for accurate control of the water temperature. The cold water is driven by a 0.37 kW water pump with an inverter to the test section with a specified water flow rate. The accuracy of water flow rate measurement by a mass flow meter is $\pm 0.2\%$.

2.4 Water loop for sub-cooler

The water loop for condensing R-134a vapor has a 200 liter constant temperature water bath equipped with a 5 kW heater and an air cooled refrigeration unit of 3 RT cooling capacity for accurate control of water temperature. A 0.37 kW water pump with an inverter is used to drive the cold water at a specified water flow rate to the sub-cooler.

2.5 Data acquisition

The data acquisition unit includes a 20 channel Fluke NetDAQ 2640A recorder combined with a personal computer. The recorder was used to record the temperature and voltage data. The NetDAQ 2640A recorder allows the measured data to transmit to personal computer to be analyzed immediately.

2.6 Experimental procedures

The vapor quality of R-134a at the test section inlet can be kept at the desired value by pre-heater. The heat transfer rate in the test section can be varied by changing the temperature and flow rate in the water loop for the test section. The flow rate of water in the test section should be high enough to have turbulent flow in the water side so that the associated single-phase heat transfer is high enough to balance the condensation heat transfer in the refrigerant side.

3. Data reduction

3.1 Two-phase condensation heat transfer

For the definition of the hydraulic diameter, Shah and Wanniarachchi[3] suggested to use two times of the channel spacing as the hydraulic diameter for plate heat exchangers when the channel width is much larger than the channel spacing. So we follow this suggestion.

$$D_h \approx 2b \tag{1}$$

The total heat transfer rate between the counter flows in the test section is calculated from the cold water side as

$$Q_t = \dot{m}_{w,c}\, c_{p,w}(T_{w,c,o} - T_{w,c,i}) \tag{2}$$

Then, the refrigerant vapor quality entering the test section is evaluated from the energy balance for the pre-heater. The heat transfer to the refrigerant in the pre-heater is the sum of the sensible heat transfer (for the temperature rise of the refrigerant to the saturated value) and latent heat transfer (for the evapo-

ration of the refrigerant).

$$Q_p = Q_{sens} + Q_{lat} \tag{3}$$

$$Q_{sens} = \dot{m}_r c_{p,r}(T_{r,sat} - T_{r,p,i}) \tag{4}$$

$$Q_{lat} = \dot{m}_r i_{fg} x_i \tag{5}$$

The above equations can be combined to evaluate the refrigerant quality at the exit of pre-heater that is considered to be the same as the vapor quality of refrigerant entering the test section. Specifically,

$$x_i = \frac{1}{i_{fg}}\left[\frac{Q_p}{\dot{m}_r} - c_{p,r}(T_{r,sat} - T_{r,p,i})\right] \tag{6}$$

The change in the refrigerant vapor quality in the test section is then deduced from the heat transfer to the refrigerant in the test section,

$$\Delta x = \frac{Q_t}{\dot{m}_r i_{fg}} \tag{7}$$

The average quality in the test section is given as

$$x_m = x_i - \frac{\Delta x}{2} \tag{8}$$

The overall heat transfer coefficient U for the counter flow between the two channels can be expressed as

$$U = \frac{Q_t}{A \cdot \Delta T_{LMTD}} \tag{9}$$

where $LMTD$ is the logarithmic mean temperature difference between the two channels defined as

$$\Delta T_{LMTD} = \frac{\Delta T_1 - \Delta T_2}{\ln(\Delta T_1 / \Delta T_2)} \tag{10}$$

where

$$\Delta T_1 = T_{r,sat,i} - T_{w,c,o} \tag{11}$$

$$\Delta T_2 = T_{r,sat,o} - T_{w,c,i} \tag{12}$$

with $T_{r,sat,i}$ and $T_{r,sat,o}$ are the saturation temperatures of R-134a corresponding respectively to the inlet and outlet pressures in the oblong shell and plate heat exchanger.

In view of the same heat transfer area in the refrigerant and water sides, the relation between the overall heat transfer coefficient and the convective heat transfer coefficients on both sides can be expressed as

$$\left(\frac{1}{h_r}\right) = \left(\frac{1}{U}\right) - \left(\frac{1}{h_{w,c}}\right) - R_{wall} A \tag{13}$$

where the modified Wilson plot method[4] was applied to calculate $h_{w,c}$.

3.2 Two-phase frictional pressure drop

To evaluate the frictional pressure drop associated with the R-134a condensation in the refrigerant channel, the frictional pressure drop Δp_f was calculated by subtracting the pressure losses at the test section inlet and exit ports Δp_{port}, then adding the deceleration pressure rise during the R-134a condensation Δp_{de} and the elevation pressure rise Δp_{ele} from the measured total pressure drop Δp_{exp} for the refrigerant channel. Note that for the vertical downward refrigerant flow studied here the elevation pressure rise should be added in evaluating Δp_f. Thus

$$\Delta p_f = \Delta p_{exp} + \Delta p_{de} + \Delta p_{ele} - \Delta p_{port} \tag{14}$$

The deceleration and elevation pressure rises were estimated by the homogeneous model for two-phase gas-liquid flow.[5]

$$\Delta p_{de} = G^2 v_{fg} \Delta x \tag{15}$$

$$\Delta p_{ele} = \frac{gL}{v_m} \tag{16}$$

where v_m is the mean specific volume of the vapor-liquid mixture in the refrigerant channel when they are homogeneously mixed and is given as

$$v_m = [x_m v_g + (1-x_m) v_f] = (v_f + x_m v_{fg}) \tag{17}$$

The pressure drop in the inlet and outlet ports was empirically suggested by Shah and Focke.[6] It is approximately 1.5 times the head due to the flow expansion at the channel inlet

$$\Delta p_{port} \approx 1.5 \left(\frac{u_m^2}{2v_m} \right) \tag{18}$$

where u_m is the mean flow velocity. With the homogeneous model, the mean velocity is

$$u_m = G v_m \tag{19}$$

Based on the above estimation, the deceleration pressure rise, the pressure losses at the test section inlet and exit ports, and the elevation pressure rise were found to be rather small. The frictional pressure drop ranges from 95~99% of the total pressure drop measured. According to the definition

$$f_{tp} \equiv -\left(\frac{\Delta p_f D_h}{2G^2 v_m L} \right) \tag{20}$$

the friction factor for the condensation of R-134a is obtained.

4. Results and discussion

4.1 Single-phase heat transfer

Before measuring the R-134a condensation heat transfer and pressure drop, single-phase water-to-water tests were conducted first.

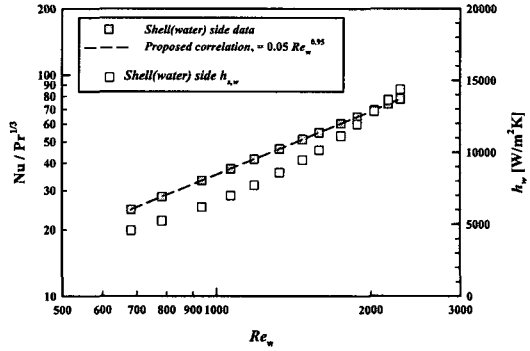

Fig. 4 Heat transfer coefficient variations with the Reynolds number for the shell side in single-phase water-to-water test.

The results from this single-phase experiment were illustrated Fig. 4 and the measured convection heat transfer coefficient in the shell side was correlated by the least square method as

$$\mathrm{Nu}_s = 0.05\ \mathrm{Re}^{0.95}\ \mathrm{Pr}^{1/3} \tag{21}$$

To estimate the uncertainty of single-phase heat transfer coefficient, an uncertainty analysis proposed by Kline and McClintock[7] was carried out. The uncertainty of single-phase heat transfer coefficient was within about ±10%.

4.2 Two-phase heat transfer

In the present investigation of the R-134a condensation in the oblong shell and plate heat exchanger, the R-134a mass flux G was varied from 40 to 80 kg/m^{2}s, the average heat flux q_w'' from 4.0 to 8.0 kW/m^2 and the saturation temperature $T_{r,sat}$ from 30 to 40℃. The measured heat transfer coefficients are to be presented in terms of their variations with the average vapor quality in the test section.

Figure 5 shows the effect of the refrigerant mass flux on the measured condensation heat transfer coefficients, where the measured data for G=40, 60 and 80 kg/m^{2}s at $T_{r,sat}$=30℃

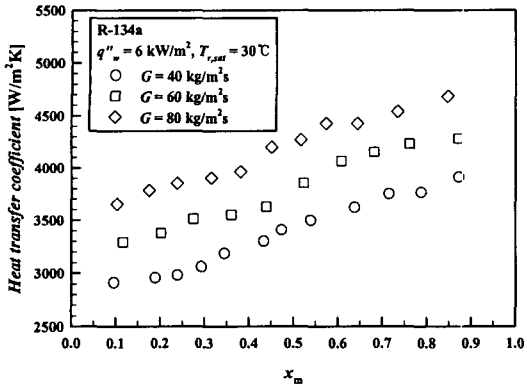

Fig. 5 Variations of condensation heat transfer coefficient with mean vapor quality for various mass fluxes at q_w'' =6.0 kW/m^2 and $T_{r,sat}$=30℃.

and q_w'' =6.0 kW/m^2 are plotted as a function of x_m. The results show that the condensation heat transfer coefficient rises linearly with the mass flux in the total vapor quality region. This obviously results from the simple fact that at a higher x_m the liquid film on the surface is thinner and the condensation rate is thus higher.

The effects of average heat flux on the condensation heat transfer are shown in Fig. 6 by plotting the measured data for q_w'' =4, 6 and 8 kW/m^2 at G=60 kg/m^{2}s and $T_{r,sat}$=30℃ as a function of x_m. It is well known that the condensation rate is almost proportional to the heat flux. The results indicate that at a given vapor quality the heat transfer coefficient is higher for a higher heat flux. Note that the R-134a quality-averaged condensation heat transfer coefficient at 8.0 kW/m^2 are about 8% larger than 4.0 kW/m^2. However, compared with the mass flux effects shown in Fig. 5, the heat flux has a small effect on the condensation heat transfer coefficient in the whole vapor quality region.

The effect of the refrigerant saturation temperature on the condensation heat transfer coefficient is illustrated in Fig. 7 by plotting the data for $T_{r,sat}$=30, 35 and 40℃ at G=60 kg/m^{2}s and q_w'' =6 kW/m^2 as a function of x_m. The results suggest that, at a given saturation temperature, the condensation heat transfer coefficient increases with the mean vapor quality. At a fixed x_m, the condensation heat transfer coefficient is lower for a higher $T_{r,sat}$ in the whole quality region. Specifically, the mean heat transfer coefficient at 30℃ is about 21% bigger than that at 40℃. This is conjectured to be mainly resulting from reduction in the conduc-

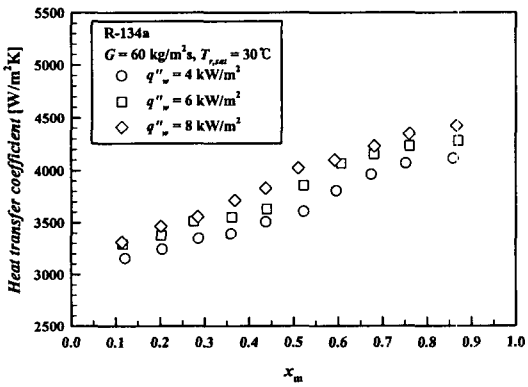

Fig. 6 Variations of condensation heat transfer coefficient with mean vapor quality for various heat fluxes at G=60 kg/m^{2}s and $T_{r,sat}$=30℃.

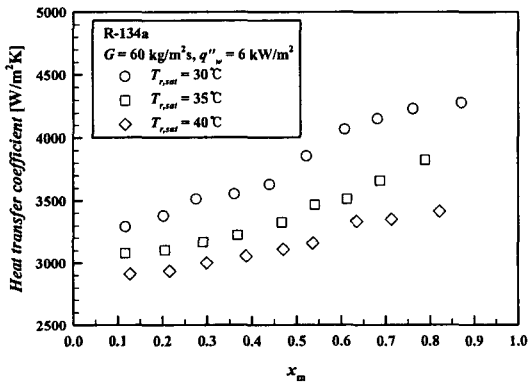

Fig. 7 Variations of condensation heat transfer coefficient with mean vapor quality for various saturation temperatures at G= 60 kg/m^{2}s and q_w'' =6.0 kW/m^2.

tivity of liquid film for the R-134a saturation temperature raised from 30 to 40℃. The associated thermal resistance of the liquid film is larger, causing a poorer heat transfer rate.

It is necessary to compare the present data for the R-134a condensation heat transfer coefficient in the oblong shell and plate heat exchanger to those in plate heat exchanger reported in the literature. Due to the limited availability of the data for plate heat exchangers with the same range of the parameters covered in the present study, the comparison is only possible for a few cases. This is illustrated in Fig. 8, in which our data are compared with correlation of Yan et al.[8] Note that the data from Yan et al. are average condensation heat transfer coefficient measured in a plate heat exchanger with the vapor quality from 0.08 to 0.86. Yan et al. proposed condensation heat transfer correlation equation such as

$$\mathrm{Nu} = \frac{h_r D_h}{k_f} = 4.118\,\mathrm{Re}_{eq}^{0.4}\,\mathrm{Pr}_f^{1/3} \qquad (22)$$

where Re_{eq} is the equivalent Reynolds number. Re_{eq} is defined as

$$\mathrm{Re}_{eq} = \frac{G_{eq} D_h}{\mu_f} \qquad (23)$$

and G_{eq} is the equivalent mass flux first proposed by Akers et al.[9] defined as

$$G_{eq} = G\left[(1-x_m) + x_m\left(\frac{\rho_f}{\rho_g}\right)^{0.5}\right] \qquad (24)$$

The comparison shows that the R-134a condensation heat transfer coefficient for oblong shell and plate heat exchanger is about 30% higher in average higher than that for the plate heat exchanger.

4.3 Two-phase pressure drop

Figure 9 shows the effect of the refrigerant mass flux on R-134a frictional pressure drop. The results indicate that, at a given mass flux, the pressure drop is larger for a higher vapor quality. In addition, the pressure drop with the vapor quality is more pronounced for a higher mass flux. This obviously results from the simple fact that at a higher x_m the velocity of vapor was larger and the pressure drop was thus higher.

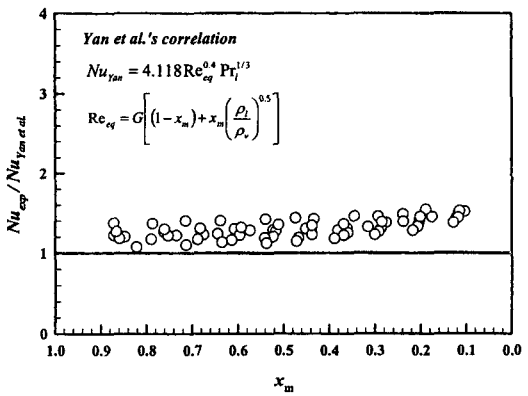

Fig. 8 Comparison of the present heat transfer data with those for plate heat exchanger from Yan et al.

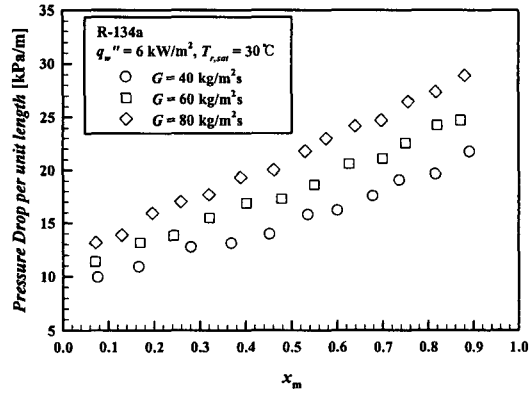

Fig. 9 Frictional pressure drop variations with the mean vapor quality for various mass fluxes at q_w'' =6.0 kW/m^2 and $T_{r,sat}$= 30℃.

Figure 10 shows the effects of the heat flux on the frictional pressure drop. The data indicate that at a given heat flux the frictional pressure drop increases linearly with the mean vapor quality of the refrigerant. But an increase in the heat flux dose not show significant effect on the frictional pressure drop.

The results in Fig. 11 for different saturation temperatures of R-134a indicated that, at a given $T_{r,sat}$, the pressure drop is larger for a higher vapor quality. Note that in the total vapor quality range the pressure drop is smaller at a higher $T_{r,sat}$. This is conjectured to be mainly resulting from a reduction in the velocity of vapor for the R-134a saturation temperature raised from 30 to 40℃.

4.4 Correlation equations

To facilitate the use of the oblong shell and plate heat exchanger as condensers, correlating equations for the dimensionless condensation

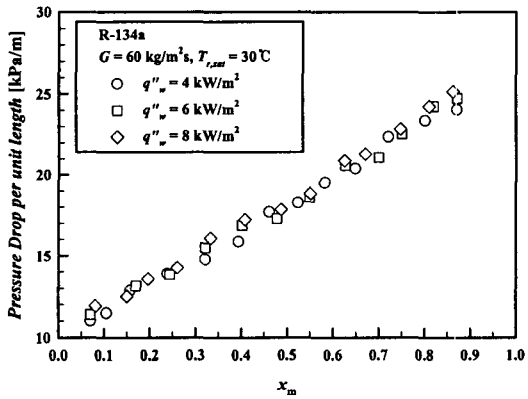

Fig. 10 Frictional pressure drop variations with the mean vapor quality for various heat fluxes at G=60 kg/m^{2}s and $T_{r,sat}$=30 ℃.

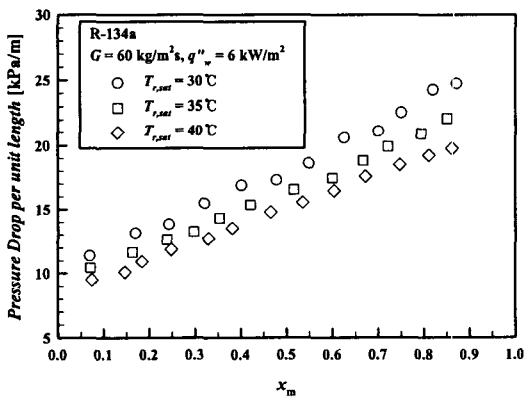

Fig. 11 Frictional pressure drop variations with the mean vapor quality for various saturation temperatures at G=60 kg/m^{2}s and q_w'' =6.0 kW/m^2.

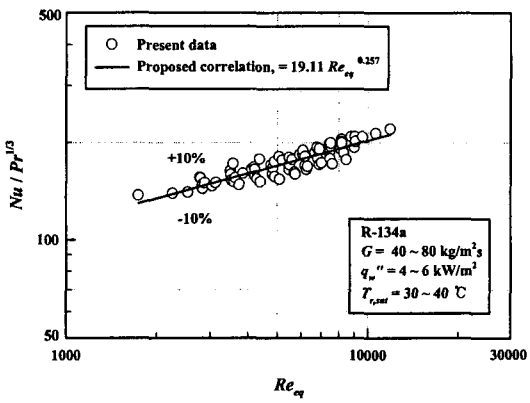

Fig. 12 Comparison of the proposed correlation for Nusselt number with the present data.

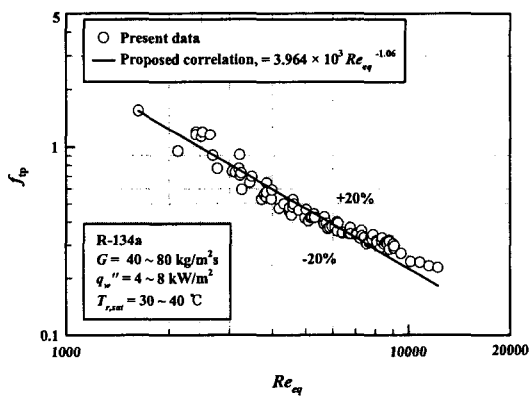

Fig. 13 Comparison of the proposed correlation for friction factor with the present data.

heat transfer coefficient and friction factor based on the present data are provided. These are the modified forms of Yan et al.'s correlations.

$$Nu = 19.11\,Re_{eq}^{0.257}\,Pr_f^{1/3} \tag{25}$$

and

$$f_{tp} = 3.964 \times 10^3\,Re_{eq}^{-1.06} \tag{26}$$

Figure 12 shows the comparison of the proposed condensation heat transfer correlation to the present data, indicating that most of the experimental values are within $\pm 10\%$. Figure 13 shows the comparison of the proposed correlation for the friction factor to the present data. It is found that the average deviation is about $\pm 20\%$ between f_{tp} correlation and the data.

5. Conclusions

An experiment has been carried out in the present study to measure the heat transfer coefficient and pressure drop for the condensation flowing in the oblong shell and plate heat exchanger. The effects of the mass flux, average imposed heat flux, saturated temperature and vapor quality on the measured data were experimentally examined in detail.

The present results for the oblong shell and plate heat exchanger show that the condensation heat transfer coefficient and pressure drop increase with the refrigerant mass flux. A rise of heat flux causes an increase in the condensation heat transfer coefficient. But the heat flux does not show effect on the frictional pressure drop. It was noted that, at a higher saturation temperature, condensation heat transfer coefficient and pressure drop are lower.

The empirical correlations are also provided for the measured heat transfer coefficients and pressure drops in terms of the Nusselt number and friction factor.

Acknowledgement

This work has been supported by Regional Research Center for Advanced Environmentally Friendly Energy Systems of Pukyong National University.

References

1. Kerner, J., Sjogren, S. and Svensson, L., 1987, Where plate exchangers offer advantages over shell-and-tube, Power, Vol. 131, pp. 53-58.
2. Williams, B., 1996, Heat transfer savings on a plate, Heating and Air Conditioning Journal, Apr., pp. 29-31.
3. Shah, R. K. and Wanniarachchi, A. S., 1992, Plate heat exchanger design theory in industry heat exchanger, in: J. M. Buchlin (ed.), Lecture Series, No. 1991-04, Von Karman Institute for Fluid Dynamics, Belgium.
4. Farrell, P., Wert, K. and Webb, R., 1991, Heat transfer and friction characteristics of turbulent radiator tubes, SAE Technical Paper series, No. 910197.
5. Collier, J. G., 1982, Convective boiling and condensation, 2nd ed., McGraw-Hill Int. Book Company, pp. 32, 90-93.
6. Shah, R. K. and Focke, W. W., 1988, Plate heat exchangers and their design theory, in: Shah, R. K., Subbarao, E. C., Mashelkar, R. A. (eds.), Heat Transfer Equipment Design, Hemisphere, Washington, DC, pp. 227-254.
7. Kline, S. J. and McClintock, F. A., 1953, Describing uncertainties in single-sample experiments, Mechanical Engineering, Vol. 75, No. 1, pp. 3-12.
8. Yan, Y.-Y., Lio, H.-C. and Lin, T.-F., 1999, Condensation heat transfer and pressure drop of refrigerant R-134a in a plate heat exchanger, Int. J. Heat and Mass Transfer 42, pp. 993-1006.
9. Akers, W. W., Dean, H. A. and Crosser, O., 1958, Condensation heat transfer within horizontal tubes, Chem. Eng. Prog. 54, pp. 89-90.